Macromolecules

Article

pubs.acs.org/Macromolecules

Covalent Capture of Self-Assembled Rosette Nanotubes

Bo-Liang Deng, Rachel L. Beingessner, Ross S. Johnson, Navdeep K. Girdhar, Christophe Danumah, Takeshi Yamazaki, and Hicham Fenniri*

National Institute for Nanotechnology, Departments of Chemistry and Biomedical Engineering, University of Alberta, 11421 Saskatchewan Drive, Edmonton, Alberta T6G 2M9, Canada

Supporting Information

ABSTRACT: Rosette nanotubes (RNTs) are self-assembled tubular architectures which have extensive chemical and physical tuning capabilities, owing to their ease of surface functionalization and flexible inner channel design. To marry these tunable features of the RNTs with the enhanced stability of a covalent polymer, here we demonstrate the covalent capture of the RNT supramolecular structure by polymerizing alkyldiamine functional groups expressed on their outer periphery in the presence of adipoyl chloride (nylon-6,6 process). The resulting polymeric materials were characterized using proton nuclear magnetic resonance spectroscopy, Fourier transform infrared spectroscopy, dynamic light scattering, and differential scanning calorimetry. Transmission and scanning electron microscopy revealed the formation of fibers and films composed of RNTs.

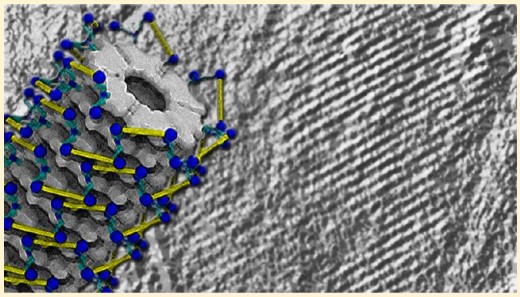

INTRODUCTION

Supramolecular polymers[1] combine the unique features of covalent polymers with the elegant design principles of self-assembly.[2] Because supramolecular polymers are built using reversible and highly directional secondary interactions between monomeric units, they benefit over traditional polymers from their tunability, recyclability, and self-healing characteristics. While these properties are a significant advantage, the caveat of their noncovalent design is their comparatively weaker architectural and dynamic stability at higher temperatures. By capturing a supramolecular structure such as a tubular assembly[3] using a polymerization process, however, the structural control and intricacy of the self-assembled polymer can be harnessed and transformed into a thermostable and processable material. Herein, we demonstrate this principle with the first reported polymerization of self-assembled rosette nanotubes (RNTs).

RNTs are discrete, biocompatible[4] tubular architectures formed in solution from a heterobicyclic molecule (G∧C) that has the Watson−Crick donor−donor−acceptor H-bonding array of guanine (G) and acceptor−acceptor−donor H-bonding array of cytosine (C).[5] The tubular structure of the RNT is comprised of stacked six-membered rosettes maintained in solution by a network of H-bonds, van der Waals, and $\pi-\pi$ stacking interactions. Detailed microscopy and spectroscopy studies have shown that these architectures have an exceptionally controlled organization that is based on these cumulatively strong and directional noncovalent interactions.[5] As well, these materials have excellent chemical and physical tuning capabilities, owing to their ease of surface functionalization with bioactive molecules,[6] inorganic complexes,[7] nanoparticles,[8] and other organic[9] moieties. By extending the length of the G∧C scaffold,[10−12] the RNT channel diameter can also be increased from 1.1 nm (bicyclic motif) to 1.4 nm (tricyclic motif)[10,12] or 1.7 nm (tetracyclic motif).[11] This results in enhanced electronic communication along the RNTs' main axis as evidenced by their J-type[13] optoelectronic properties.[12]

Because of the RNTs design flexibility, polymerization of their supramolecular structure provides a strategy to synthesize many novel covalent polymers. To this end, here we describe the synthesis and self-assembly of **3a** and **3b** (Figure 1) into RNTs expressing alkyl triamine groups on their outer surface and utilize these as sites for polymerization based on the nylon-6,6 process.[14] Details pertaining to the structure, thermostability, and morphology of the resulting RNT polymer materials **4a** and **4b** are provided using ^{1}H NMR spectroscopy, FTIR spectroscopy, dynamic light scattering (DLS), differential scanning calorimetry (DSC), scanning electron microscopy (SEM), and transmission electron microscopy (TEM).

RESULTS AND DISCUSSION

In applying the synthetic strategy previously developed for functionalizing the G∧C motif,[5,9] the synthesis of RNT polymers **4a** and **4b** began by coupling aldehyde **1**[5a] to amine **2a** or **2b** using a reductive amination reaction (Figure 1). Deprotection under acidic conditions (95:5, TFA:thioansiole, v:v) then provided **3a** and **3b** as the TFA salts in excellent yields of 82% and 95%, respectively. The structures of these G∧C monomers were confirmed by ^{1}H NMR, HRMS, elemental analysis, and FTIR. Subsequent self-assembly of motifs **3a** and **3b** (1 mg/mL) in water generated the respective

Received: June 24, 2012
Revised: August 10, 2012
Published: August 22, 2012

dx.doi.org/10.1021/ma3012976 | Macromolecules 2012, 45, 7157−7162

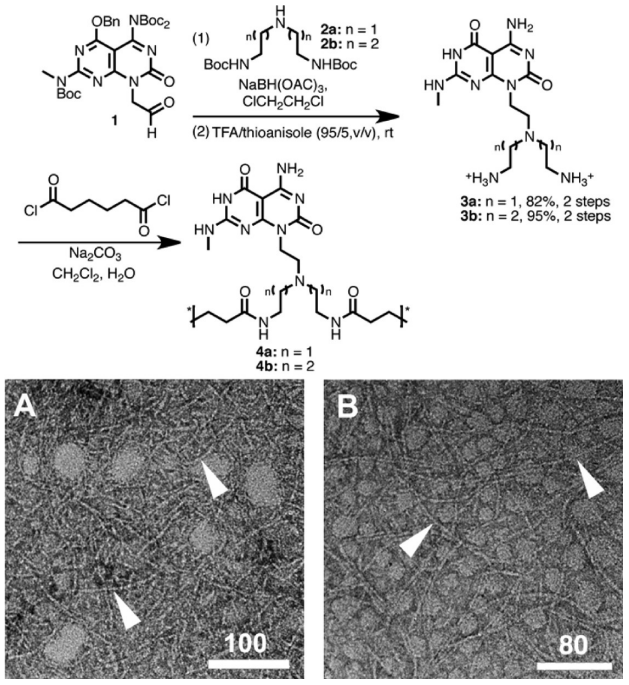

Figure 1. Synthesis of polymers **4a** and **4b** (top) and negatively stained TEM images of RNTs assembled in water from **3a** (A) and **3b** (B). White arrows point to individual RNTs; scale bars in nm.

RNTs having average diameters of 3.4 ± 0.2 nm as determined by TEM (Figure 1).

Interfacial polycondensation based on the nylon-6,6 synthesis[14] was next carried out using the respective nanotube solutions. Specifically, a solution of **3a** (or **3b**) (1 mg/mL) in water was treated with Na_2CO_3, cooled to 0 °C, and then added dropwise to an ice-cooled solution of adipoyl chloride in dichloromethane. The polymerization occurred immediately at the interface of the two solvents to yield polyamides **4a** and **4b**. The films formed were recovered and washed with hot water, acetone, and methanol to remove unreacted starting material.

^{1}H NMR spectroscopy, FTIR spectroscopy, and DLS were used to establish the formation of polymers **4a** and **4b**. The ^{1}H NMR spectra of **4a** obtained in deuterated trifluoroacetic acid displayed the methylene protons of the adipoyl moiety on the polymer backbone, the methylene protons connecting the G∧C base to the polymer, and the methyl group on the G-face of the motif (Figure S2). The relative integrations of these ^{1}H NMR peaks suggested that the polymerization was quantitative. FTIR analysis further confirmed this polymerization since the ammonium groups stretching bands (3600−2300 cm^{-1}) assigned to the ethylamines of **3a** were replaced by CH stretchings attributed to the polymer backbone of **4a**. Additional secondary amide I bands and CH_2 scissoring bands with increased intensity were also evident for **4a** (Figure S1).

In the case of polymer **4b**, the presence of a ^{1}H NMR peak characteristic of a methylene α to an ammonium group suggested that the polymerization occurred mainly on one of the primary amines (Figure S3). Although ammonium group stretching bands (3700−2200 cm^{-1}) could not be conclusively identified in the FTIR spectra of **4b** to confirm this (because of overlapping signals), the absorption between 3700 and 2800 cm^{-1} was much stronger than that observed for **4a**. Regardless, the presence of CH stretchings and additional secondary amide I and II bands and CH_2 scissoring bands were supportive of at least the partial polymerization of **3b**.

Subsequent DLS studies of RNTs **3a** and **3b** in water (1 mg/mL, 25 °C) resulted in well-equilibrated structures, which were evident by the narrow unimodal size distributions (Figure 2A,B). The average hydrodynamic diameters of these materials

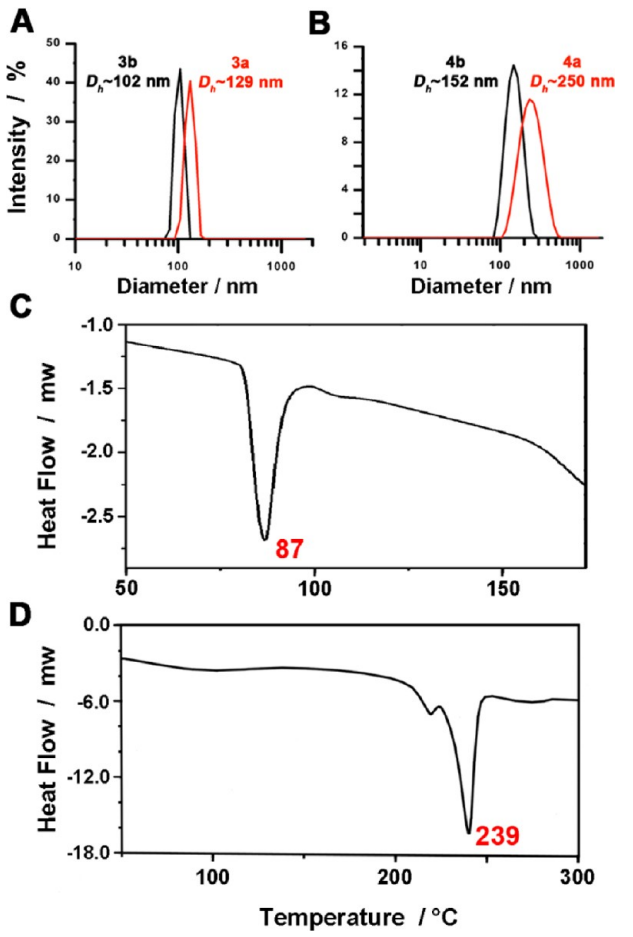

Figure 2. DLS of (A) **3a** and **3b** in water and (B) **4a** and **4b** in MeCN (1 mg/mL, 25 °C); DSC of **3b** (C) and **4b** (D) performed on the solid materials at a heating rate of 10 °C/min.

were determined to be 129 and 102 nm, respectively, which indicates that **3a** forms slightly larger aggregates. DLS measurements of **4a** and **4b** (1 mg/mL, 25 °C, carried out in acetonitrile for solubility reasons) gave larger average hydrodynamic diameters of 250 and 152 nm, respectively. Although the hydrodynamic dimensions of polymerized and non-polymerized RNT samples were obtained in different solvents, and thus may not be directly comparable, the significantly larger diameter and polydispersity of **4a** and **4b** are in agreement with the polymerization of the RNTs.

Using DSC, the thermal behaviors of **3a** and **3b** were next compared to the polymerized materials **4a** and **4b**, respectively. In the case of **3a** (functionalized with the ethylene triamine moiety), the absence of a melting transition in the range of 50−270 °C (data not shown) suggested an amorphous state for this material. In contrast, the corresponding polymerized solid **4a** had two broad melting transitions around 108 and 185 °C (Figure S10), suggesting the presence of two broad polymer states or populations, possibly with intra- and inter-RNT

dx.doi.org/10.1021/ma3012976 | Macromolecules 2012, 45, 7157−7162

connectivities. However, given the broadness of the peaks, meaningful enthalpies could not be determined.

Interestingly, compound **3b** (functionalized with the propylene triamine moiety) displayed a single melting transition at 87 °C (Figure 2C), which is reminiscent of the solution melting temperature previously reported for RNTs functionalized with lysine amino acids[5a] and thus suggests that **3b** forms RNTs with similar thermal stability in the solid state as well. In comparison, the melting profile of the corresponding polymer **4b** (Figure 2D) featured an intense endothermic transition at a much higher temperature of 239 °C, which is similar to nylon-6,6 (255−265 °C).[15] The measured enthalpies of endotherms (ΔH_m) for compounds **3b** and **4b** are 4.59 and 50.1 J/g, respectively. While crystalline nylon-6,6 has a much higher ΔH_m value (197 J/g),[16] a lower degree of polymerization[17] or crystallinity[18] decreases it to ca. of 53−61 J/g. As this is the range where the ΔH_m of **4b** is (50.1 J/g), this result is in agreement with the NMR data suggesting incomplete polymerization.

Thus, on the basis of DLS and DSC results, it was concluded that the RNTs underwent surface-initiated polymerization leading to the covalent capture and stabilization of the RNTs with varying degrees of polymerization depending on their surface functionalities.

SEM and TEM images of **4a** (Figure 3 and Figures S6 and S8) and **4b** (Figure 4 and Figures S7 and S9) revealed the formation of thin films as well as fibrous materials and provided insight into the organization of the polymer network. In particular, the images in Figure 3D (and Figure S8D) show polymer **4a** in a parallel tape-like formation in which the RNTs are aligned along their main axis. The average distance between consecutive RNTs was measured to be 3.4 ± 0.2 nm, which is in excellent agreement with the calculated average diameter for the nonpolymerized RNT (**3a**). This alignment suggests that the well-dispersed, protonated RNTs form bundles and tapes prior to polymerization as a result of their neutralization with Na_2CO_3 in the course of the polymerization reaction. Polymerization thus likely occurs along the length of the RNTs as well as between adjacent nanotubes. Overall, this demonstrates that the self-assembled RNT architecture is indeed maintained and captured during the polymerization process and that, moreover, this strategy holds substantial promise for the design of novel polymeric materials with unique hierarchical architecture.

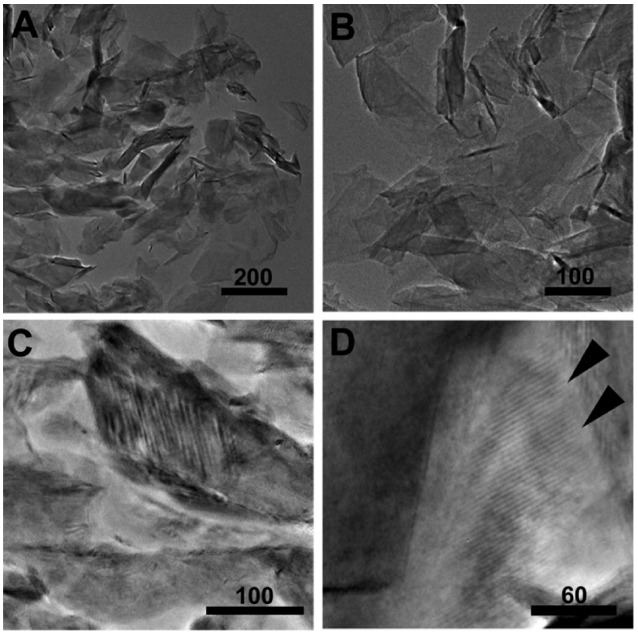

Figure 3. TEM images of **4a** (1 mg/mL in MeCN) showing the formation of thin films made up of RNTs. The parallel tape-like formation of the RNTs is seen in image D. Scale bars in nm.

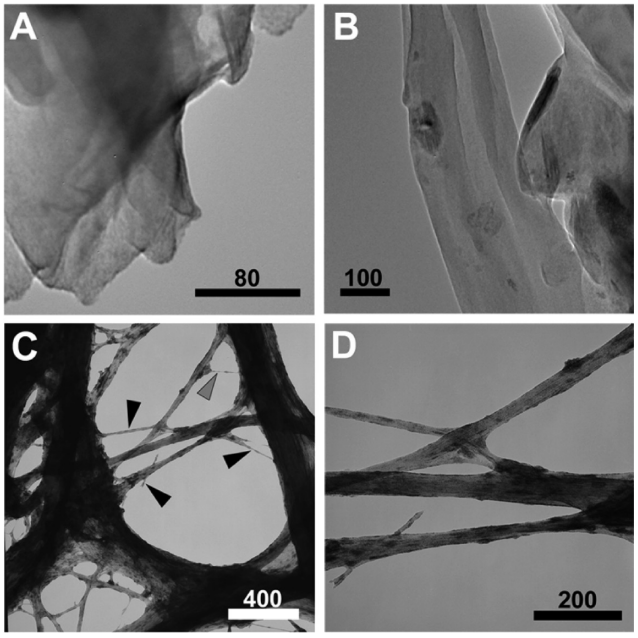

Figure 4. TEM images of **4b** (1 mg/mL in MeCN) showing the formation of thin films (A, B) and fibrous materials (C, D). Black arrows in image C point to RNT bundles; gray arrow points to a single RNT. Scale bars in nm.

Using the minimized molecular model of RNTs **3a** shown in Figure 5, the accessible polymerization connections between the nitrogen labeled N1 on a given G∧C motif and the neighboring N1 or N2 atoms on a different motif within the same nanotube were examined. Given that the measured carbonyl-to-carbonyl length of adipoyl chloride in the all-trans configuration is ca. 6.5 Å, and that upon polymerization the bond length between the carbonyl carbon of the adipoyl moiety and N1 would be ca. 1.4 Å, we can roughly predict that neighboring N atoms at a distance of ca. 9.3 Å from N1 shown in yellow could be bridged together. N-to-N1 (or N2) distances represented in orange are not within a favorable range for cross-linking with adipoyl chloride assuming these length restrictions. On this basis, adjacent rosettes as well as alternating rosettes can be covalently linked via the adipoyl tether in many different combinations (Figure S13). Although the example in Figure 5C is idealized, it provides insight into the bridging of N1−N1 and N2−N2 atoms between adjacent rosettes.

■ CONCLUSION

In summary, we have demonstrated the covalent capture of self-assembled RNTs using a polymerization strategy based on nylon-6,6 methodology. Specifically, ethylene and propylene diamine groups expressed on the outer RNT surface were polymerized using adipoyl chloride under basic conditions. The resulting materials were characterized by ^{1}H NMR, FTIR, DSC, DLS, and electron microscopy techniques. DSC established our main aim, which is an enhanced thermostability of polymer **4b**

dx.doi.org/10.1021/ma3012976 | Macromolecules 2012, 45, 7157−7162

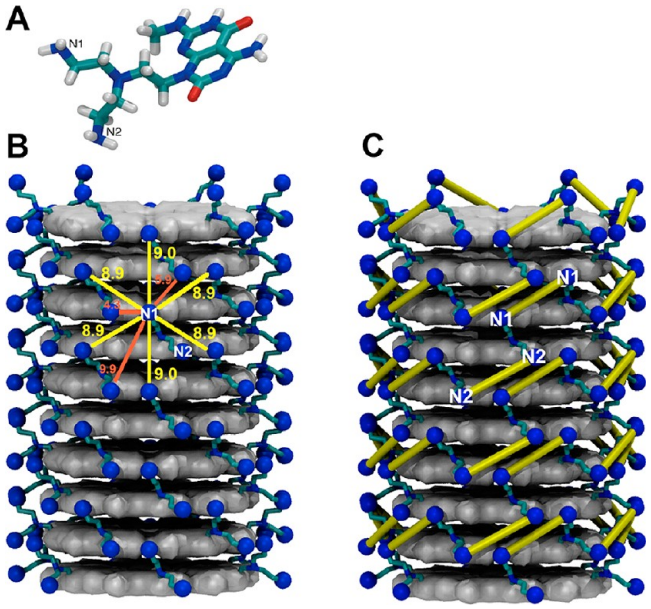

Figure 5. Molecular models of RNT **3a** illustrating one possible mode of cross-linking within the nanotube. (A) Compound **3a** with nitrogen atoms labeled N1 and N2. (B) Distances (Å) from N1 on a motif to neighboring N1 or N2 on a different motif. An atom-to-atom length of ca. 9.3 Å (marked in yellow) is optimal for two amines (N1−N1 or N2−N2) to be linked to adipoyl chloride given an all-trans configuration. N-to-N distances represented in orange are not within an appropriate range for polymerization with adipoyl chloride. (C) Example of an N1−N1, N2−N2 connectivity of **3a** through the adipoyl tether.

compared to the corresponding supramolecular system **3b**. TEM imaging confirmed that the RNT architecture is preserved to some extent during the polymerization process and that the polymer network has substantial organization, which is based on the alignment and cross-linking of adjacent RNTs. With our ability to tailor the physical and chemical properties of the RNTs including their inner channels and surface functional groups, we envision that a variety of new RNT covalent polymers with unique physical and chemical properties could be generated.

EXPERIMENTAL SECTION

All commercial chemicals were used as purchased without further purification. NMR characterizations were performed on a 300−600 MHz spectrometers in the specified deuterated solvents (D_2O, trifluoracetic acid-*d*, $CDCl_3$). The NMR data are presented as follows: chemical shift, assignment, coupling, integration.

FTIR was performed on a Nicolet Nic-Plan IR microscope equipped with a MCT-A detector attached to a Nicolet Magna 750 FTIR. The spectra were acquired from 4000 to 650 cm^{-1} using 128 scans at 4 cm^{-1} resolution and Nicolet Omnic software.

SEM and TEM samples were prepared by floating a carbon-coated 400-mesh copper grid on a droplet of a 1 mg/mL solution of **3a** or **3b** (in water) or **4a** or **4b** (in MeCN) for 10 s. Excess material was blotted with filter paper at the edge of the grid. Negative staining (for TEM) was performed by floating the grids on a drop of 1% uranyl acetate in water for 10 s and blotting excess staining agent. The samples were dried overnight at room temperature prior to imaging. SEM images were obtained at 1.0 kV accelerating voltage and a working distance of 1.0−2.0 mm on a high-resolution Hitachi S4800 cold field emission SEM. TEM imaging was performed on a JEOL 2010 microscope operated at 200 kV.

DLS experiments were performed using a Malvern Zetasizer Nano S working at a 173° scattering angle at 25 °C. This instrument is equipped with a 40 mW He−Ne laser (λ = 633 nm) and an Avalanche photodiode detector. Solutions (1 mg/mL) were prepared and then filtered through a Whatman 0.45 μm pore diameter PVFD membrane filter prior to measurement.

DSC was performed on a DSC1000 differential calorimeter (TA Instruments) fitted with a liquid nitrogen cooling system. The samples were placed in hermetically sealed DSC pans and then heated and cooled at rates of 10 and 5 °C, respectively. A first heating scan was performed to erase the thermal history of the materials. DSC measurements were then obtained in the second heating scan. In all cases, the endotherms were reversible.

Synthesis of 2a. A solution of diethylenetriamine (0.43 g, 4.2 mmol) and triethylamine (1.8 mL, 13 mmol) in THF (10 mL) was cooled to 0 °C and stirred under a nitrogen atmosphere. A solution of 2-(*tert*-butoxycarbonyloxyimino)-2-phenylacetonitrile (2.1 g, 8.3 mmol) in THF (40 mL) was then added over a period of 1 h. The mixture was stirred at 0 °C for 2.5 h, followed by 2 h at room temperature. The solvent was removed under reduced pressure (rotavap) to provide a light yellow oil, which was redissolved in CH_2Cl_2 (120 mL) and washed with an aqueous solution of 5% NaOH (2 × 40 mL). The organic layer was further washed with dH_2O (50 mL) and brine (35 mL), dried over anhydrous Na_2SO_4, and concentrated under reduced pressure (rotavap). Purification by silica gel chromatography (10% MeOH/CH_2Cl_2) provided 1.22 g of compound **2a** ($C_{14}H_{29}N_3O_4$, 97%) as a colorless solid. ^{1}H NMR (300 MHz, $CDCl_3$) δ (ppm): 4.85 (brs, 2H), 3.15−3.25 (m, 4H), 2.71 (t, ^3J = 6.0 Hz, 4H), 1.65 (brs, 1H), 1.43 (m, 18H). CI-MS: expected for $(M + H^+)/z$: 304; observed: 304 ($(M + H)^+/z$, 100%).[19]

Synthesis of 3a. Amine **2a** (0.5 g, 0.78 mmol) was added to a solution of aldehyde **1**[5a] (237 mg, 0.78 mmol in 1,2-dichloroethane (20 mL) under a N_2 atmosphere. After stirring for 6 h, $Na(OAc)_3BH$ (196 mg, 0.93 mmol) was added. The reaction mixture was then stirred at rt under N_2 for 36 h before being quenched with H_2O and extracted with $CHCl_3$ (200 mL). The organic layer was subsequently washed with 10% citric acid solution (50 mL), dH_2O (50 mL), 5% $NaHCO_3$ (50 mL), and brine (50 mL), dried over anhydrous Na_2SO_4, filtered, and concentrated under reduced pressure (rotavap). Purification by flash chromatography over silica gel (20% EtOAc/hexane) provided the protected coupled G∧C base as a white foam (0.61 g, $C_{45}H_{69}N_9O_{12}$, 84% yield). ^{1}H NMR ($CDCl_3$, 400 MHz) δ (ppm): 7.45−7.32 (m, 5H), 5.56 (s, 2H), 5.14 (brs, 2H), 4.37 (t, J = 7.6 Hz, 2H), 3.46 (s, 3H), 3.18 (d, J = 5.6 Hz, 4H), 2.81 (t, J = 7.6 Hz, 2H), 2.68 (t, J = 5.6 Hz, 4H), 1.57 (s, 9H), 1.43 (s, 18H), 1.32 (s, 18H). ^{13}C NMR ($CDCl_3$, 100 MHz) δ (ppm): 165.9, 161.4, 161.2, 160.6, 156.4, 155.9, 152.5, 149.5, 135.1, 128.8−128.6, 93.2, 84.0, 83.2, 79.2, 70.3, 54.3, 51.2, 41.4, 39.0, 35.2, 28.7, 28.3, 28.1. Positive ESI-MS: expected for $(M + H)^+/z$: 928.5; observed: 928.8 ($(M + H)^+/z$, 100%). Positive high-resolution ESI-MS: expected for $(M + Na)^+/z$: 950.4958; observed: 950.4958.

Trifluoroacetic acid and thioanisole (95:5 v/v, 10 mL) were added to the protected coupled G∧C base (0.61 g, 0.657 mmol) and stirred at rt under a N_2 atmosphere for 72 h. Diethyl ether (20 mL) was then added to precipitate the product, which was collected by centrifugation, washed with diethyl ether (10 mL), and dried under reduced pressure (rotavap) to provide **3a** as a white solid (444 mg, $C_{13}H_{23}N_9O_2$ + 3(CF_3COOH) + H_2O, 97%). ^{1}H NMR (400 MHz, D_2O) δ (ppm): 4.32−4.28 (t, J = 8.0 Hz, 2H), 3.15−3.12 (t, J = 6.4 Hz, 4H), 3.05 (s, 3H), 2.98−2.90 (m, 6H). ESI-MS: expected for $(M + H)^+/z$: 338.2; observed: 338.2 ($(M + H)^+/z$, 100%). Positive high-resolution ESI-MS: expected for $(M + H)^+/z$: 338.2048; observed: 338.2049. Elemental analysis: calculated for [$C_{13}H_{23}N_9O_2$ + 3(CF_3COOH) + H_2O]: C: 32.72; H: 4.05; N: 18.07; found: C: 32.98; H: 4.19; N: 18.02.

Synthesis of 4a. A solution of adipoyl chloride (27 μL, 0.19 mmol) in CH_2Cl_2 (10 mL) was treated with an ice-cold solution of **3a** (50 mg, 0.15 mmol) and Na_2CO_3 (16 mg, 0.15 mmol) in dH_2O (5 mL) using a syringe. The polymerization occurred immediately (without stirring) at the interface of the two solvents. The resulting **4a**

dx.doi.org/10.1021/ma3012976 | *Macromolecules* 2012, 45, 7157−7162

was then removed from solution and washed with hot dH_2O (10 mL), acetone (10 mL), and methanol (10 mL). ^1H NMR (trifluoroacetic acid-*d*, 400 MHz): δ (ppm) 3.34−3.22 (Me, brs, 3H), 2.72−2.54 ($C_{b+c+d}H$, brs, 6H), 2.00−1.78 ($C_{a+e+f}H$, brs, 6H), 1.58−1.30 ($C_{g+i}H$, m, 4H), 0.98−0.80 ($C_{h+j}H$, m, 4H).

Synthesis of 2b. A solution of bis(3-aminopropyl)amine (0.28 g, 2.1 mmol) and triethylamine (0.88 mL, 6.3 mmol) in THF (10 mL) was cooled to 0 °C and stirred under a N_2 atmosphere. A solution of 2-(*tert*-butoxycarbonyloxyimino)-2-phentylacetonitrile (1.04 g, 4.19 mmol) in THF (20 mL) was then added over 30 min. The mixture was stirred at 0 °C for 3 h then 1 h at rt. The solvent was then removed under reduced pressure (rotavap) to yield a yellow oil which was dissolved in CH_2Cl_2 (100 mL) and washed with an aqueous solution of 5% NaOH (2 × 40 mL). The organic layer was subsequently washed with dH_2O (50 mL) and brine (50 mL), dried over anhydrous Na_2SO_4 and then concentrated *in vacuo* to provide **2b** as a white solid (0.71 g, $C_{16}H_{33}N_3O_4$, quant) as a white solid. ^1H NMR (300 MHz, $CDCl_3$) δ (ppm): 5.14 (brs, 2H), 3.18 (m, 4H), 2.63 (t, ^3J = 6.6 Hz, 4H), 1.65 (brs, 1H), 1.62 (m, 4H), 1.42 (s, 18H). EI-MS: expected for $(M + H)^+/z$: 332.3; observed: 332.3 ($(M + H)^+/z$, 1.2%), 57.10 ($C_4H_9^+/z$, 100%). CI-MS: expected for $(M + H^+)/z$: 332.3; observed: 331.9 ($[M + H]^+/z$, 100%).[20]

Synthesis of 3b. Amine **2b** (0.52 g, 1.56 mmol) was added to a solution of aldehyde **1**[5a] (1.0 g, 1.6 mmol) and DIPEA (0.41 mL, 2.3 mmol) in 1,2-dichloroethane (25 mL) under a N_2 atmosphere. After stirring for 10 min, $Na(OAc)_3BH$ (393 mg, 1.86 mmol) was added. The reaction mixture was then stirred at rt for 36 h under N_2 atmosphere before being quenched with H_2O and extracted with $CHCl_3$ (200 mL). The organic layer was subsequently washed with 10% citric acid solution (50 mL), dH_2O, 5% $NaHCO_3$ (50 mL), and brine (50 mL), dried over anhydrous Na_2SO_4, filtered, and then concentrated under reduced pressure (rotavap). Purification by flash chromatography over silica gel (20% EtOAc/hexane) provided the protected coupled G∧C base **3b** as a white solid (1.42 g, $C_{47}H_{73}N_9O_{12}$, 95% yield). ^1H NMR ($CDCl_3$, 500 MHz) δ (ppm): 7.45−7.36 (m, 5H), 5.59 (s, 2H), 5.23 (brs, 2H), 4.42 (t, *J* = 6.5 Hz, 2H), 3.47 (s, 3H), 3.18−3.08 (m, 4H), 2.77 (t, *J* = 6.5 Hz, 2H), 2.56 (t, *J* = 6.5 Hz, 4H), 1.65−1.60 (m, 4H), 1.60 (s, 9H), 1.44 (s, 18H), 1.35 (s, 18H). ^{13}C NMR ($CDCl_3$, 125 MHz) δ (ppm): 165.7, 161.1, 161.0, 160.3, 156.1, 155.7, 152.4, 149.4, 134.9, 128.6−127.8, 92.9, 83.8, 83.0, 78.8, 70.1, 52.0, 50.7, 40.8, 39.0, 34.9, 28.5, 28.2, 27.8, 27.6. Positive ESI-MS: expected for $(M + H)^+/z$: 956.5; observed: 956.5 ($(M + H)^+/z$, 100%). Positive high-resolution ESI-MS: expected for $(M + H)^+/z$: 956.5452; observed: 956.5447.

Trifluoroacetic acid and thioanisole (95:5 v/v, 10 mL) were added the protected coupled G∧C base (1.20 g, 1.25 mmol) and stirred at rt under a nitrogen atmosphere for 72 h. Diethyl ether (20 mL) was then added to precipitate the product, which was collected by centrifugation, washed with diethyl ether, and dried under reduced pressure to provide 1.04 g of **3b** ($C_{15}H_{27}N_9O_2$ + 4(CF_3COOH) + H_2O, 99%). ^1H NMR (400 MHz, D_2O) δ (ppm): 4.49−4.46 (t, *J* = 6.4 Hz, 2H), 3.49−3.46 (t, *J* = 6.4 Hz, 2H), 3.32−3.28 (m, 4H), 3.00−2.96 (m, 4H), 2.91 (s, 3H), 2.07−1.98 (m, 4H). Positive ESI-MS: expected for $(M + H)^+/z$: 366.2; observed: 366.3 ($(M + H)^+/z$, 100%). Positive high-resolution ESI-MS: expected for $(M + H)^+/z$: 366.2366; observed: 366.2368. Elemental analysis: calculated for [$C_{15}H_{27}N_9O_2$ + 4(CF_3COOH) + H_2O]: C: 32.90; H: 3.96; N: 15.02; found: C: 32.77; H: 4.07; N: 14.64.

Synthesis of 4b. A solution of adipoyl chloride (0.02 mL, 0.14 mmol) in CH_2Cl_2 (10 mL) was treated with an ice-cold solution of **3b** (50 mg, 0.14 mmol) and Na_2CO_3 (19 mg, 0.14 mmol) in dH_2O (5 mL) using a syringe. The polymerization occurred immediately (without stirring) at the interface of the two solvents. The resulting **4b** was then removed from solution and washed with hot dH_2O (10 mL), acetone (10 mL), and methanol (10 mL). ^1H NMR (trifluoroacetic acid-*d*, 400 MHz) δ (ppm): 3.56−3.48 (C_gH, brs, 2H), 3.37−3.20 (Me, brs, 3H), 2.80−2.43 ($C_{b+c+d}H$, m, 6H), 2.16−1.70 ($C_{a+h+e}H$, m, 6H), 1.65−1.25 ($C_{f+i}H$, m, 4H), 1.05−0.83 (C_jH, m, 2H).

■ ASSOCIATED CONTENT

Ⓢ Supporting Information

FTIR, NMR, additional microscopy images, DSC, and molecular modeling. This material is available free of charge via the Internet at http://pubs.acs.org.

■ AUTHOR INFORMATION

Corresponding Author

*Tel 780-641-1750; Fax 780-641-1601; e-mail hicham.fenniri@ualberta.ca.

Notes

The authors declare no competing financial interest.

■ ACKNOWLEDGMENTS

We thank Canada's National Research Council and Natural Science and Engineering Research Council, Canada Foundation for Innovation, the National Institute for Nanotechnology, and the University of Alberta for supporting this work.

■ REFERENCES

(1) (a) Brunsveld, L.; Folmer, B. J. B.; Meijer, E. W.; Sijbesma, R. P. *Chem. Rev.* **2001**, *101*, 4071−4097. (b) Palmer, L. C.; Stupp, S. I. *Acc. Chem. Res.* **2008**, *41*, 1674−1684. (c) Ciferri, A. *Macromol. Rapid Commun.* **2002**, *23*, 511−529. (d) Palmer, L. C.; Stupp, S. I. *Acc. Chem. Res.* **2008**, *41*, 1674−1684. (e) Lehn, J.-M. *Polym. Int.* **2002**, *51*, 825−839. (f) De Greef, T. F. A.; Smulders, M. M. J.; Wolffs, M.; Schenning, A. P. H. J.; Sijbesma, R. P.; Meijer, E. W. *Chem. Rev.* **2009**, *109*, 5687−5754. (g) Bouteiller, L. *Adv. Polym. Sci.* **2007**, *207*, 79−112. (h) Armstrong, G.; Buggy, M. *J. Mater. Sci.* **2005**, *40*, 547−559. (i) Fox, J. D.; Rowan, S. J. *Macromolecules* **2009**, *42*, 6823−6835. (j) Zimmerman, N.; Moore, J. S.; Zimmerman, S. C. *Chem. Ind.* **1998**, 604−610.

(2) (a) Lehn, J.-M. *Supramolecular Chemistry*; VCH: Weinheim, 1995. (b) Lehn, J.-M. *Angew. Chem., Int. Ed. Engl.* **1990**, *29*, 1304−1309. (c) Elemans, J. A. A. W.; Rowan, A. E.; Nolte, R. J. M. *J. Mater. Chem.* **2003**, *13*, 2661−2670.

(3) (a) Perino, A.; Schmutz, M.; Meunier, S.; Mesini, P. J.; Wagner, A. *Langmuir* **2011**, *27*, 12149−12155. (b) Kim, Y.; Mayer, M. F.; Zimmerman, S. C. *Angew. Chem.* **2003**, *115*, 1153−1158. (c) Ouhib, F.; Bugnet, E.; Nossov, A.; Bonardet, J.-L.; Bouteiller, L. *Polymer* **2010**, 3360−3364. (d) Huang, K.; Rzayev, J. *J. Am. Chem. Soc.* **2009**, *131*, 6880−6885. (e) Barboiu, M.; Cerneaux, S.; van der Lee, A.; Vaughan, G. *J. Am. Chem. Soc.* **2004**, *126*, 3545−3550. (f) Kim, Y.; Mayer, M. F.; Zimmerman, S. C. *Angew. Chem., Int. Ed.* **2003**, *42*, 1121−1126. (g) Stewart, S.; Liu, G. *Angew. Chem., Int. Ed.* **2000**, *39*, 340−344. (h) Beginn, U.; Zipp, G.; Möller. *Adv. Mater.* **2000**, *12*, 510−513. (i) Zhou, M.; Kidd, T. J.; Noble, R. D.; Gin, D. L. *Adv. Mater.* **2005**, *17*, 1850−1853.

(4) (a) Journeay, W. S.; Suri, S. S.; Moralez, J. G.; Fenniri, H.; Singh, B. *Small* **2008**, *4*, 817−823. (b) Journeay, W. S.; Suri, S. S.; Moralez, J. G.; Fenniri, H.; Singh, B. *Small* **2009**, *5*, 1446−1452. (c) Journey, W. S.; Suri, S. S.; Moralez, J. G.; Fenniri, H.; Singh, B. *Int. J. Nanomed.* **2008**, *3*, 373−383.

(5) (a) Fenniri, H.; Deng, B. L.; Ribbe, A. E. *J. Am. Chem. Soc.* **2002**, *124*, 11064−11072. (b) Moralez, J. G.; Raez, J.; Yamazaki, T.; Motkuri, R. K.; Kovalenko, A.; Fenniri, H. *J. Am. Chem. Soc.* **2005**, *127*, 8307−8309. (c) Fenniri, H.; Deng, B. L.; Ribbe, A. E.; Hallenga, K.; Jacob, J.; Thiyagarajan, P. *Proc. Natl. Acad. Sci. U. S. A.* **2002**, *99*, 6487−6492. (d) Raez, J.; Moralez, J. G.; Fenniri, H. *J. Am. Chem. Soc.* **2004**, *126*, 16298−16299. (e) Fenniri, H.; Mathivanan, P.; Vidale, K. L.; Sherman, D. M.; Hallenga, K.; Wood, K. V.; Stowell, J. G. *J. Am. Chem. Soc.* **2001**, *123*, 3854−3855. (f) Yamazaki, T.; Fenniri, H.; Kovalenko, A. *ChemPhysChem* **2010**, *11*, 361−367. (g) Marsh, A.; Silvestri, M.; Lehn, J.-M. *Chem. Commun.* **1996**, 1527−1528. (h) Mascal, M.; Hext, N. M.; Warmuth, R.; Moore, A. H.; Turkenburg, J. P. *Angew. Chem., Int. Ed.* **1996**, *108*, 2203−2206.

(6) (a) Chun, A. L.; Moralez, J. G.; Webster, T. J.; Fenniri, H. *Biomaterials* **2005**, *26*, 7304−7309. (b) Chun, A. L.; Moralez, J. G.; Fenniri, H.; Webster, T. J. *Nanotechnology* **2004**, *15*, S234−S239. (c) Zhang, L.; Rodriguez, J. R.; Myles, A. J.; Fenniri, H.; Webster, T. J. *Nanotechnology* **2009**, *20*, 175101. (12 p). (d) Zhang, L.; Rakotondradany, F.; Myles, A. J.; Fenniri, H.; Webster, T. J. *Biomaterials* **2009**, *30*, 1309−1320. (e) Zhang, L.; Ramsaywack, S.; Fenniri, H.; Webster, T. J. *Tissue Eng., Part A* **2008**, *14*, 1353−1364. (f) Zhang, L.; Chen, Y.; Rodriguez, J.; Fenniri, H.; Webster, T. J. *Int. J. Nanomed.* **2008**, *3*, 323−333. (g) Chen, Y.; Pareta, R. A.; Bilgen, B.; Myles, A. J.; Fenniri, H.; Ciombor, D. M.; Aaron, R. K.; Webster, T. J. *Tissue Eng., Part C* **2010**, *16*, 1233−1243. (h) Zhang, L.; Hemraz, U. D.; Fenniri, H.; Webster, T. J. *J. Biomed. Mater. Res., Part A* **2010**, *95A*, 550−563. (i) Fine, E.; Zhang, L. J.; Fenniri, H.; Webster, T. J. *Int. J. Nanomed.* **2009**, *4*, 91−97. (j) Song, S.; Chen, Y.; Yan, Z.; Fenniri, H.; Webster, T. J. *Int. J. Nanomed.* **2011**, *6*, 101−107. (k) Chen, Y.; Song, S.; Yan, Z.; Fenniri, H.; Webster, T. J. *Int. J. Nanomed.* **2011**, *6*, 1035−1044. (l) Alshamsan, A.; El-Bakkari, M.; Fenniri, H. *Mater. Res. Soc. Symp. Proc.* **2011**, *2010*, 1316−1319. (m) Suri, S. S.; Rakotondradani, F.; Myles, A. J.; Fenniri, H.; Singh, B. *Biomaterials* **2009**, *30*, 3084−3090. (n) Suri, S. S.; Mills, S.; Aulakh, G. K.; Rakotondradany, F.; Fenniri, H.; Singh, B. *Int. J. Nanomed.* **2011**, *6*, 3113−3123. (o) Le, M. H. A.; Suri, S. S.; Rakotondradany, F.; Fenniri, H.; Singh, B. *Vet. Res.* **2010**, *41*, 75.

(7) Alsbaiee, A., St.; Jules, M.; Beingessner, R. L.; Cho, J.-Y.; Yamazaki, T.; Fenniri, H. *Tetrahedron Lett.* **2012**, *53*, 1645−1651.

(8) Chhabra, R.; Moralez, J. G.; Raez, J.; Yamazaki, T.; Cho, J.-Y.; Myles, A. J.; Kovalenko, A.; Fenniri, H. *J. Am. Chem. Soc.* **2010**, *132*, 32−33.

(9) (a) Tikhomirov, G.; Oderinde, M.; Makeiff, D.; Mansouri, A.; Lu, W.; Heirtzler, F.; Kwok, D. Y.; Fenniri, H. *J. Org. Chem.* **2008**, *73*, 4248−4251. (b) Tikhomirov, G.; Yamazaki, T.; Kovalenko, A.; Fenniri, H. *Langmuir* **2008**, *24*, 4447−4450. (c) Beingessner, R. L.; Deng, B.-L.; Fanwick, P. E.; Fenniri, H. *J. Org. Chem.* **2008**, *73*, 931−939. (d) Beingessner, R. L.; Diaz, J. A.; Hemraz, U. D.; Fenniri, H. *Tetahedron Lett.* **2011**, *52*, 661−664.

(10) Borzsonyi, G.; Johnson, R. S.; Myles, A. J.; Cho, J.-Y.; Yamazaki, T.; Beingessner, R. L.; Kovalenko, A.; Fenniri, H. *Chem. Commun.* **2010**, *46*, 6527−6529.

(11) Borzsonyi, G.; Alsbaiee, A.; Beingessner, R. L.; Fenniri, H. *J. Org. Chem.* **2010**, *75*, 7233−7239.

(12) Borzsonyi, G.; Beingessner, R. L.; Yamazaki, T.; Cho, J.-Y.; Myles, A. J.; Malac, M.; Egerton, R.; Kawasaki, M.; Ishizuka, K.; Kovalenko, A.; Fenniri, H. *J. Am. Chem. Soc.* **2010**, *132*, 15136−15139.

(13) Kuhn, H.; Kuhn, C. In *J Aggregates*; Kobayashi, T., Ed.; World Scientific: Singapore, 1996.

(14) (a) Angelo, R. J.; Miura, H.; Gardner, K. H.; Chase, D. B.; English, A. D. *Macromolecules* **1989**, *22*, 117−121. (b) Leblanc, J. P.; Jois, Y. H. R.; Gibson, H. W. *Macromolecules* **1992**, *25*, 6752−6755.

(15) Braun, E.; Levin, B. C. *Fire Mater.* **1987**, *11*, 71−88.

(16) Brandrup, J.; Immergut, E. H. *Polymer Handbook*, 3rd ed.; Wiley: New York, 1989.

(17) (a) Costa, G.; Meli, D.; Song, Y.; Turturro, A.; Valenti, B.; Castellano, M.; Falqui, L. *Polymer* **2001**, *42*, 8035−8042. (b) Castellano, M.; Nebbia, D.; Turturro, A.; Valenti, B.; Costa, G.; Falqui, L. *Macromol. Chem. Phys.* **2002**, *203*, 1614−1624. (c) Garcia-Ramirez, M.; Cavaille, J. Y.; Dupeyre, D.; Peguy, A. *J. Polym. Sci., Part B: Polym. Phys.* **1994**, *32*, 1437−1448.

(18) Lu, H.; Xu, X.; Li, X.; Zhang, Z. *Bull. Mater. Sci.* **2006**, *29*, 485−490.

(19) The characterization of compound **2a** is in agreement with the literature data. Westerberg, D. A.; Carney, P. L.; Rogers, P. E.; Kline, S. J.; Johnson, D. K. *J. Med. Chem.* **1989**, *32*, 236−243.

(20) The characterization of compound **2b** is in agreement with the literature data. Marsh, I. R.; Bradley, M. *Tetrahedron* **1997**, *53*, 17317−17334.